Processing of 3-Ketoacyl-CoA Thiolase by the Peroxisomal Protease DEG15

Nirali Shah
Biology Honors Thesis
Program in Biology
The University of Michigan
April 1, 2015

Sponsor: Laura J. Olsen, Ph.D.

Readers:
Amy Chang, Ph.D.
Anuj Kumar, Ph.D.

Undergraduate Honors Thesis

Processing of 3-Ketoacyl-CoA Thiolase by the Peroxisomal Protease DEG15

Nirali Shah

Table of Contents

ABSTRACT

Peroxisomes are small, membrane-bound organelles found in virtually all eukaryotic cells. They play an important role in breaking down hydrogen peroxide in the cell and in β-oxidation of fatty acids. Peroxisomal proteins are synthesized in the cytosol and post-translationally transported into the peroxisome. There are two peroxisomal targeting signals (PTS) that are known to aid in the transport of matrix proteins; the PTS1 is located at the carboxyl terminus of the protein and the PTS2 is located at the amino terminus. Upon entry of the protein into the peroxisome, the PTS2 is typically cleaved off by the peroxisomal protease DEG15 (in plants) or by TYSND1 (in mammals). In this study, thiolase (THL) is examined in *Arabidopsis thaliana* (At) and *Zea mays* (Zm) to determine whether DEG15 processing is conserved across species. I used AtDEG15 and ZmDEG15 in protease assays with ZmTHL and AtTHL to determine whether the proteases had different efficiencies with different substrates and whether homologous enzyme/substrate pairs have higher processing levels. Protease assays performed *in vitro* demonstrated that ZmTHL and AtDEG15 seem to be the most efficient enzyme/substrate pair. There is a Cys in many PTS2 proteins that is thought to be required for processing. Site-directed mutagenesis of the Cys in ZmTHL showed that the removal of and the substitution of the Cys for Gly significantly decreased, and occasionally obliterated processing. These results indicate that the conserved Cys or the protein conformation around the conserved Cys is likely to play an important role in DEG15 recognition and processing.

INTRODUCTION

Peroxisomes are small, membrane-enclosed organelles found in virtually all eukaryotic cells. These organelles, which are approximately 1 μm in diameter, are visible under the electron microscope and are sometimes referred to as microbodies (Donaldson et al., 2001). As of today, not much research has been done on these organelles, although their functions are essential to the survival of cells. Peroxisomes contain at least 50 different enzymes, which function in a variety of biochemical pathways in different types of cells. Originally, peroxisomes were defined as organelles that carry out oxidation reactions, leading to the production of hydrogen peroxide. Since hydrogen peroxide is harmful to the cell, peroxisomes contain the enzyme catalase, which decomposes hydrogen peroxide either by converting it to water or by using it to oxidize another compound. Many different substrates are catabolized by similar oxidative reactions in peroxisomes, including uric acid, amino acids, and fatty acids. Peroxisomes are responsible for the catabolism of very long-chain fatty acids through β-oxidation, which provides a major source of metabolic energy. In animal cells, fatty acids are oxidized in both peroxisomes and mitochondria, however, in some yeasts and plants, fatty acid oxidation is restricted to peroxisomes (Cooper, 2000).

Peroxisomes are also involved in lipid biosynthesis. In animal cells, cholesterol and dolichol are synthesized in the peroxisome and the endoplasmic reticulum (Cooper, 2000). Peroxisomes aid in the synthesis of bile acids in the liver, which are derived from cholesterol. Peroxisomes also contain enzymes necessary for the synthesis of plasmologens, a family of phospholipids in which one of the hydrocarbon chains is joined to glycerol by an ether bond rather than an ester bond (Cooper, 2000).

In higher plants, at least four classes of peroxisomes have been identified: leaf peroxisomes, glyoxysomes, root nodule peroxisomes, and unspecialized peroxisomes (Donaldson et al., 2001). All classes of peroxisomes have a single membrane and have a finely granular matrix. Leaf peroxisomes are involved in photorespiration, which serves to metabolize glycolate, a side product formed during photosynthesis (Hu et al., 2012). The first step of the Calvin cycle entails the addition of CO_2 to ribulose-1,5-bisphosphate, yielding two molecules of 3-phosphoglycerate. The enzyme ribulose-1,5-bisphosphate carboxylase (Rubisco) sometimes catalyzes the addition of O_2 instead of CO_2, producing one molecule of 3-phosphoglycerate and one molecule of phosphoglycolate. Phosphoglycolate is first converted to glycolate and then transferred to peroxisomes, where it is oxidized and converted to glycine. Glycine is then transported to the mitochondria, where two molecules of glycine are converted to one molecule of serine, with the loss of CO_2 and NH_3. The serine returns to the peroxisome and is converted to glycerate. Finally, the glycerate is transported back to the chloroplasts where it reenters the Calvin cycle. Through photorespiration, peroxisomes play an important role by allowing most of the carbon in glycolate to be recovered and utilized (Hu et al., 2012).

Glyoxysomes are a particular type of peroxisome found only in plants, particularly in the fat storage tissues of germinating seeds. Glyoxysomes are responsible for the conversion of stored fatty acids to carbohydrates, which provides energy and raw materials for growth of the germinating plant. Glyoxysomes carry out these functions through the glyoxylate cycle (Hayashi et al., 2014). The glyoxylate cycle is an anabolic pathway converting acetyl-CoA into succinate, and is catalyzed by malate synthase, malate dehydrogenase, isocitrate lyase, citrate synthase, and aconitase (Hayashi et al.,

2014). This process is one of the distinguishing factors between glyoxysomes and other peroxisomes.

Root nodule peroxisomes exist in the root nodules of certain legumes and are involved in nitrogen metabolism (Donaldson et al., 2001). In several tropical legumes, nitrogen is transported in the form of ureides, allantoin, and allantoic acid. Ureide biosynthesis takes place in several subcellular compartments. The conversion of urate to allantoin, one of the last steps of the biosynthesis pathway, is catalyzed by urate oxidase in the peroxisomes (Donaldson et al., 2001).

Finally, unspecialized peroxisomes exist in plant tissues that do not partake in photosynthesis and that lack storage of lipids, such as the roots of most plants. They tend to have a smaller size, lower frequency, and lower density compared to glyoxysomes and leaf-type peroxisomes (Donaldson et al., 2001). There is not much known about their specific role in cellular metabolism.

Proteins that control peroxisome assembly, division, and inheritance are named peroxins (encoded by *PEX* genes). Over a dozen peroxins are conserved from yeasts to mammals and are essential for normal human development (Ma et al., 2011). Many peroxisome biogenesis disorders (PBDs) in humans, including Zellweger syndrome spectrum (ZSS) and rhizomelic chondrodysplasia punctata (RCDP) type I, are caused by a loss of certain peroxins (Waterham and Ebberink, 2012). Mutations in the *PEX7* gene are responsible for RCDP, whereas mutations in any one of the other *PEX* genes cause the ZSS disorders. Children born with ZSS lack functional peroxisomes and have a life expectancy of six to seven months (Crane et al., 2005).

Unlike mitochondria and chloroplasts, peroxisomes lack their own DNA and ribosomes. Thus all peroxisomal proteins are encoded by nuclear genes, synthesized on ribosomes free in the cytosol, and then incorporated into pre-existing peroxisomes (Lodish et al., 2000). Two different peroxisomal targeting signals (PTSs) have been characterized in the trafficking of matrix proteins from the cytosol into the peroxisome. The PTS1 consists of a tripeptide located at the carboxyl terminus of the protein and the PTS2 is a nonapeptide located 20-30 residues from the amino terminus (Ma et al., 2011).

The PTS1 sequence closely approximates Ser-Lys-Leu-COO- or a similar sequence (Ma et al., 2011). PTS1-containing proteins in the cytoplasm are recognized posttranslationally by the receptor protein Pex5p and taken to the protein complex on the peroxisome (Figure 1). At this site, the PTS1 protein is given entry into the lumen of the peroxisome (Gatto et al., 2000). After the cargo protein has entered the peroxisome, Pex5p is recycled back into the cytosol to perform multiple rounds of entry into the peroxisome matrix (Dammai and Subramani, 2001).

The PTS2 constitutes a nonapeptide with the sequence (R/K)-(L/V/I/Q)-X-X-(L/V/I/H/Q)-(L/S/G/A/K)-X-(H/Q)-(L/A/F) near the amino terminus of a protein (Ma et al., 2011). Delivery of PTS2 proteins to peroxisomes requires the PTS2 receptor, Pex7p (Figure 1). Once in the peroxisome, proteolytic enzymes—DEG15 in plants and TYSND1 in mammals—in the matrix of the peroxisome cleave the targeting signal of many, but not all, PTS2 proteins (Helm et al., 2007; Kurochkin et al., 2007). Processing of the PTS2 upon protein import is conserved in higher eukaryotes (Schuhmann et al., 2008). The cleavage site typically contains a cysteine (Schuhmann et al., 2008). However, in lower eukaryotes, such as yeasts, a PTS2 is present at the amino terminus of

many mature proteins (Schuhmann et al., 2008). Therefore, it is clear that processing is not conserved across all eukaryotes.

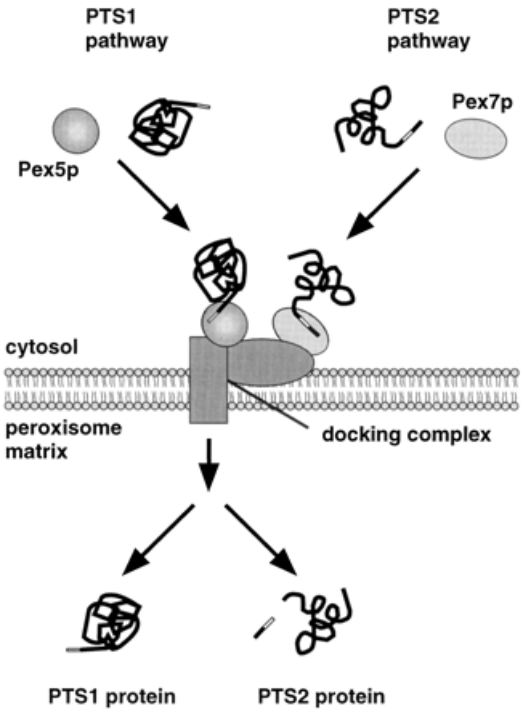

Figure 1: Model for import of PTS1- and PTS2-containing proteins. PTS1-containing proteins are recognized by the receptor protein Pex5p, and PTS2-containing proteins interact with the receptor protein Pex7p. These protein complexes are then brought to the docking station on the membrane of the peroxisome, and the proteins are translocated into the matrix. Upon entry into the peroxisome, the PTS2 is removed proteolytically. Taken from Johnson and Olsen (2001).

In higher plants, DEG15 is the proteolytic enzyme that cleaves the PTS2 pre-sequence from the protein (Helm et al., 2007). Depending on Ca^{2+} addition, DEG15 can be either shifted to a 72 kDa monomer or a 144 kDa dimer. The dimer is responsible for removing the PTS2 pre-sequence, whereas the monomer is a general protease activated by denatured proteins (Helm et al., 2007). It has not yet been proven that the cysteine on the PTS2 protein is the recognition site for DEG15 to cleave the protein. The biological relevance of removing part of the protein has yet to be determined. Similarly, in mitochondria and chloroplasts, most proteins imported begin as precursors containing

amino acids at the amino terminus that are not present in the mature protein. These residues comprise one or more targeting sequences that direct the protein to its proper destination within the organelle. Except in the case of outer-membrane proteins, the targeting sequences are removed from the remainder of the polypeptide chain, leaving the mature protein sequence (Lodish et al., 2000).

3-ketoacyl CoA thiolase (THL) is an enzyme involved in the mevalonate pathway as well as the β-oxidation of fatty acids (Figure 2). This protein catalyzes the final step of fatty acid oxidation in which acetyl-CoA is released and the CoA ester of a fatty acid two carbons shorter is formed. In *Arabidopsis thaliana*, expression of the thiolase gene is known to be required for the efficient mobilization of triacylglycerol during germination and seedling development (Footitt et al., 2007). The PTS2 of AtTHL is readily cleaved by AtDEG15 through *in vitro* protease assays (Olsen Lab, unpublished results).

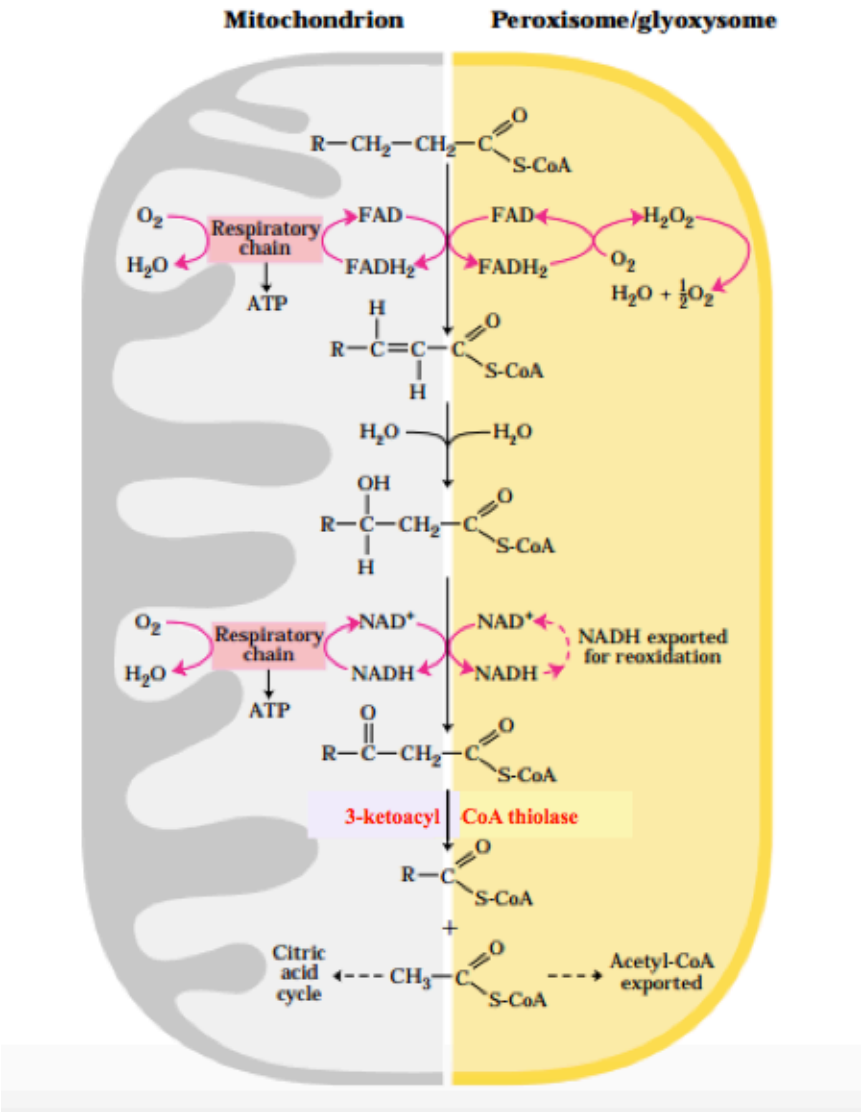

Figure 2: Comparison of β-oxidation in animal mitochondria and in plant peroxisomes. Two major differences are highlighted in this diagram; the electrons from $FADH_2$ are transferred directly to O_2 in the peroxisome. Additionally, the NADH produced during β-oxidation cannot be oxidized and these reducing equivalents are exported out of the peroxisome to the cytosol. 3-ketoacyl-CoA thiolase is shown here to catalyze the last step of β-oxidation, producing acyl-CoA and acetyl-CoA. In mitochondria, acetyl-CoA is further oxidized in the citric acid cycle. In peroxisomes, acetyl-CoA is exported for reuse in biosynthetic reactions. Image adapted from Nelson et al., (2008).

At present, there has been little work done to investigate processing of THL in *Zea mays* by AtDEG15 or ZmDEG15. It is unclear whether processing and DEG15 recognition is conserved across various eukaryotic species. Additionally, little research

has been done to determine where exactly within the amino acid sequence of the PTS2 protein is the site of recognition and cleavage by DEG15. The purpose of this study was to determine if AtDEG15 and ZmDEG15 *in vitro* could process ZmTHL and to determine, through site-directed mutagenesis, if the conserved Cys in ZmTHL could be involved in processing by DEG15. This information is useful to help understand peroxisomal biogenesis and functions, and help understand PTS2-specific diseases, such as rhizomelic chondrodysplasia punctata.

RESULTS

Analysis of THL Peroxisomal Targeting Signal

To examine the amino acid sequences of AtTHL and ZmTHL near their processing sites, protein alignments were generated using Clustal Omega's Multiple Sequence Alignment tool (https://www.ebi.ac.uk/Tools/msa/clustalo/). The purpose of these alignments was to determine which residues were conserved between different homologs of thiolase and to compare the amino acid sequences of various PTS2-containing proteins. The proteins in Figure 3 were chosen to examine because of their PTS2 signals and conserved cysteines, which appeared to be conserved across different homologs of some proteins. Only a partial sequence alignment, which contains the PTS2 signal and a conserved cysteine, is shown (Figure 3). From these alignments, it is apparent that the conserved cysteine is present in many PTS2-containing proteins. This observation led to the hypothesis that the cysteine might play a role in protein processing by DEG15. Both thiolase homologs contain the PTS2 signal, RQ-x_5-HL, and have an overall alignment with 77% sequence identity (Figure S1).

```
ZmTHL  RQRVLLAHLLPSPSAA-SSQPQ----LAASACAAGDSAAYQRSSSFGDDVVVVAAYRT
AtTHL  RQRVLLEHLRPSSSSSHNYEAS----LSASACLAGDSAAYQRTSLYGDDVVIVAAHRT

ZmPMDH     RMATLASHLRHPSVSHPQMEDVPLLRGSNCRAKGAAPGFKVAILGAAGG
AtPMDH1    RIARISAHLNPPN-LHNQIADGSGLNRVACRAKGGSPGFKVAILGAAGG
AtCSY2     RLAVLTAHLAVSDTVGLEQVLPAIAPWCTSAHITAAPHGSLKG
AtACX3     RAHVLANHILQSNPPS-SNPSLSRELCL-QYSPPELNESYGFDVK
AtLACS6    RIARISAHLNPPNLHNQIADGSGLNRVACRAKGGSPGFK
```

Figure 3: Alignment of amino acid sequences near DEG15 processing sites using ClustalW. ZmTHL and AtTHL are shown to display conserved PTS2 signals and a conserved cysteine. Residues in green indicate PTS2 signals. Residues in red indicate putative conserved cysteines. ZmPMDH, *Zea mays* malate dehydrogenase; AtPMDH1, *Arabidopsis thaliana* malate dehydrogenase 1; CSY2, citrate synthase 2; ACX3, acyl-CoA oxidase 3; LACS6, long-chain acyl-CoA synthetase.

Processing of AtTHL and ZmTHL by AtDEG15 and ZmDEG15

Thus, to investigate the processing of AtTHL and ZmTHL by AtDEG15 and ZmDEG15, standard protease assays were performed. It would be interesting to note whether the proteases had different efficiencies with different proteins, and whether or not homologous enzyme/substrate pairs have higher processing. Radioactively labeled AtTHL and ZmTHL were incubated with 10 µg of either AtDEG15 or ZmDEG15 *in vitro* at 37°C for 4 hours, separated by SDS-PAGE, and visualized by autoradiography (Figure 4).

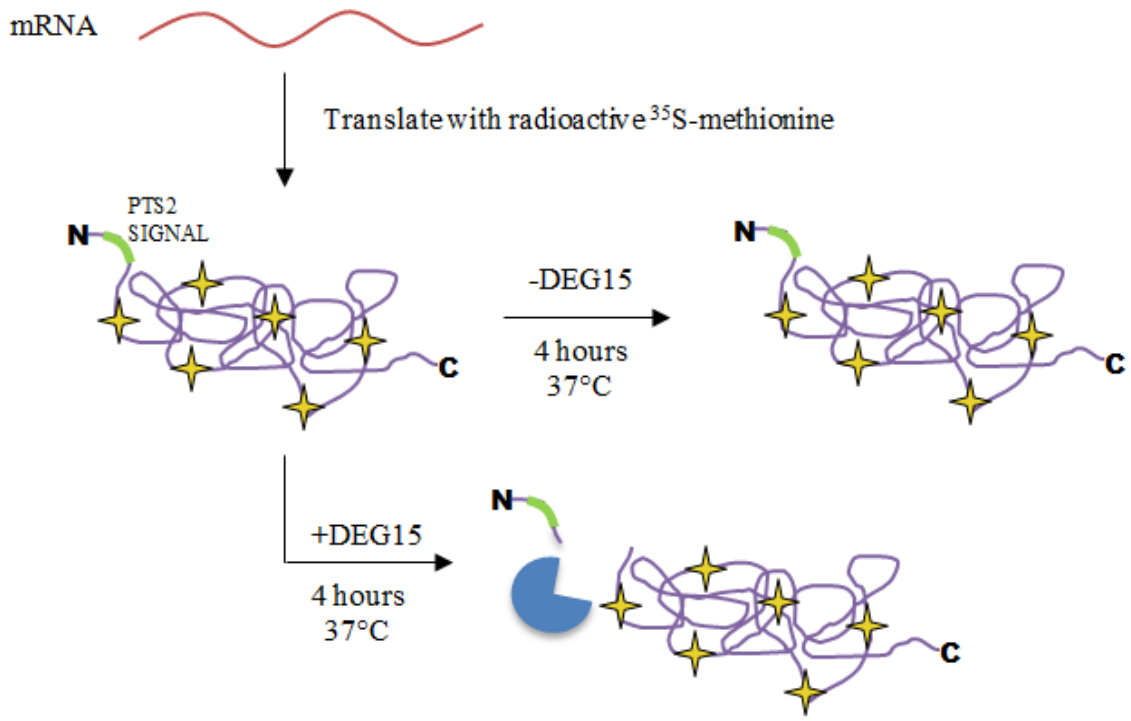

Figure 4: Schematic of a DEG15 Protease Assay with PTS2 proteins. The protein is first synthesized with radioactively labeled ^{35}S-methionine in a cell-free wheat germ extract. The radioactively labeled residues are represented by the yellow stars. The PTS2 signal is indicated near the N-terminus of the protein. The protein is then incubated either in the presence or absence of DEG15 for 4 hours at 37°C. In the presence of DEG15, the PTS2 signal should be cleaved. The results are analyzed by SDS-PAGE and quantified with a phosphor-screen using a Personal Molecular Imager® FX and Quantity One Quantitation Software.

Processing was evident in all assay samples regardless of the substrate and protease homologs present (Figure 5). The processed, or mature band, in samples containing ZmTHL and AtTHL lanes (denoted mZmTHL and mAtTHL) appeared around 44 kDa, just beneath that of the full-length proteins (48 kDa and 48.6 kDa respectively), as expected (Figure 5A). Overall, the processing of ZmTHL was strongest in the presence of AtDEG15 (Figure 5B). Quantification indicated 44% processing of ZmTHL by AtDEG15 (Figure 5B). Upon repeating this assay 3 times, the results consistently showed ZmTHL to be more efficiently processed than AtTHL, and AtDEG15 to be a more efficient protease (Figure 5B). Therefore, processing appears to occur similarly between enzymes and substrates of these two species.

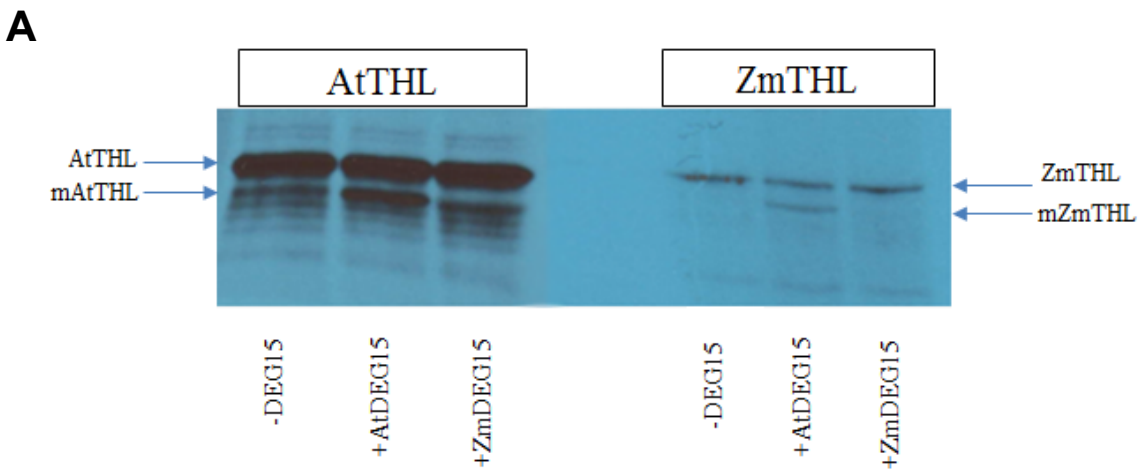

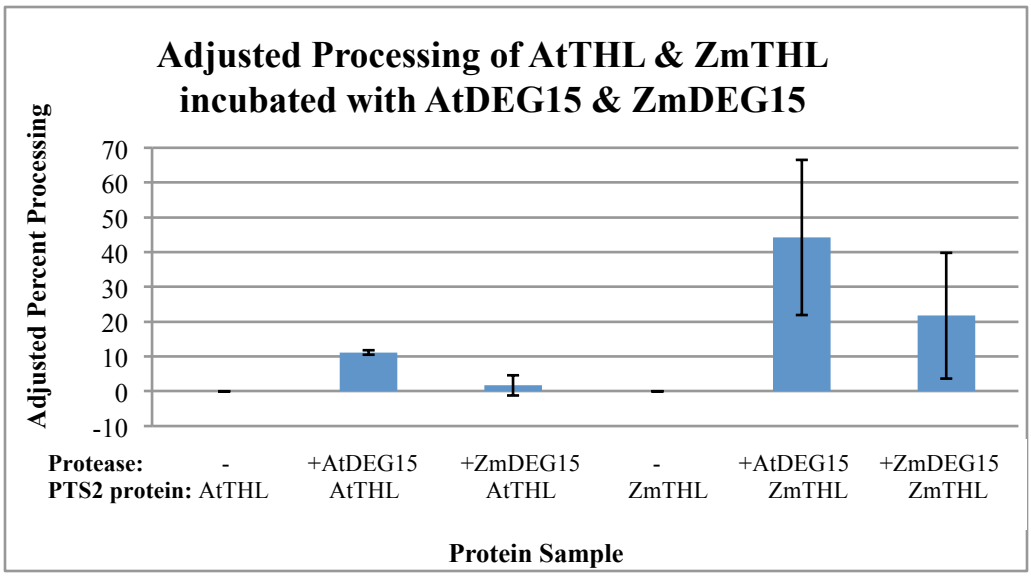

Figure 5: (A) One of three protease assays of ZmTHL and AtTHL and (B) quantification of the results of all three assays. Protease assays were repeated three times with AtDEG15 and ZmDEG15 under the same conditions: 10 µg DEG15 was incubated with 250,000 cpm radioactively labeled THL for 4 hours at 37°C; 50,000 cpm loaded per lane; 3-night exposure. Blue bars represent the averages of the three protease assays. Error bars represent the standard error from the three protease assays. Adjusted percent processing refers to the percent processing after subtracting the percent processing of the negative control.

Processing of ZmTHL Mutants by AtDEG15

Using the most efficient processing enzyme/substrate pair, the next question was whether the conserved cysteine of ZmTHL (indicated in Figure 3) is involved in DEG15 recognition and processing. Site-directed mutagenesis was utilized to construct a substitution and a deletion mutant (Figure 6). The C33G mutant refers to a glycine being substituted for the conserved cysteine. The C33Δ mutant indicates the conserved cysteine has been deleted. ZmTHL wild type, ZmTHL C33G, and ZmTHL C33Δ were incubated with AtDEG15, in standard DEG15 protease assays.

```
ZmTHL:        1- MEKAIDRQRVLLAHLLPSPSAASSQPQLAASACAAGDSAA -40
ZmTHL C33G:   1- MEKAIDRQRVLLAHLLPSPSAASSQPQLAASAGAAGDSAA -40
ZmTHL C33Δ:   1- MEKAIDRQRVLLAHLLPSPSAASSQPQLAASA-AAGDSAA -40
```

Figure 6: ZmTHL mutant constructs. The above constructs were made by site-directed mutagenesis. Red residues show the mutated cysteine residue; this conserved cysteine may be necessary for processing by DEG15. Green residues form the PTS2 signal.

Overall, the processing of the mutants was weak compared to that of the wild-type protein. The processed band in ZmTHL wild type appeared at roughly 44 kDa, the expected size as the mature protein should be slightly smaller than the unprocessed band, reflecting cleavage of the PTS2 signal (Figure 7A). The processed bands in ZmTHL C33G and ZmTHL C33Δ were considerably lighter, however, they also appeared to be at the expected size. The quantitative data in Figure 7B is derived from the gel in Figure 7A, as processing for ZmTHL wild type was 19%, while processing of the mutants was considerably less. From these results, it can be noted that the cysteine is important and

necessary in DEG15 processing. By deleting the cysteine or mutating it to a glycine, processing was negatively impacted as compared to ZmTHL wild type (Figure 7B).

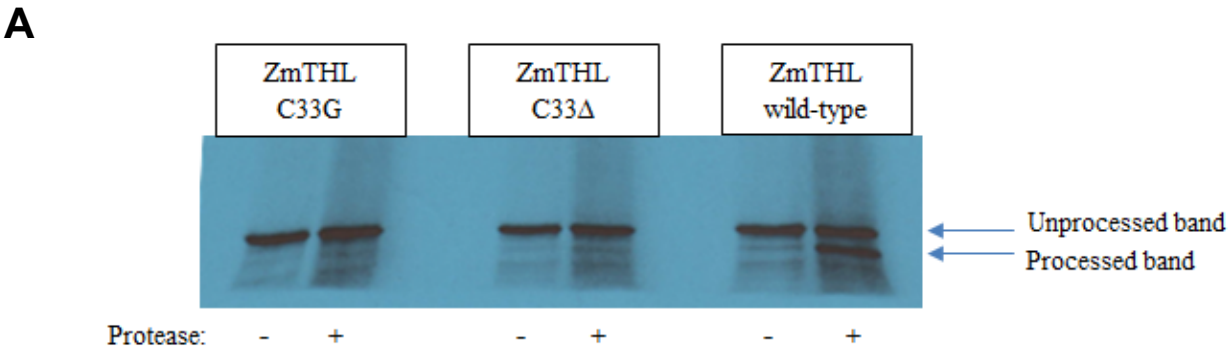

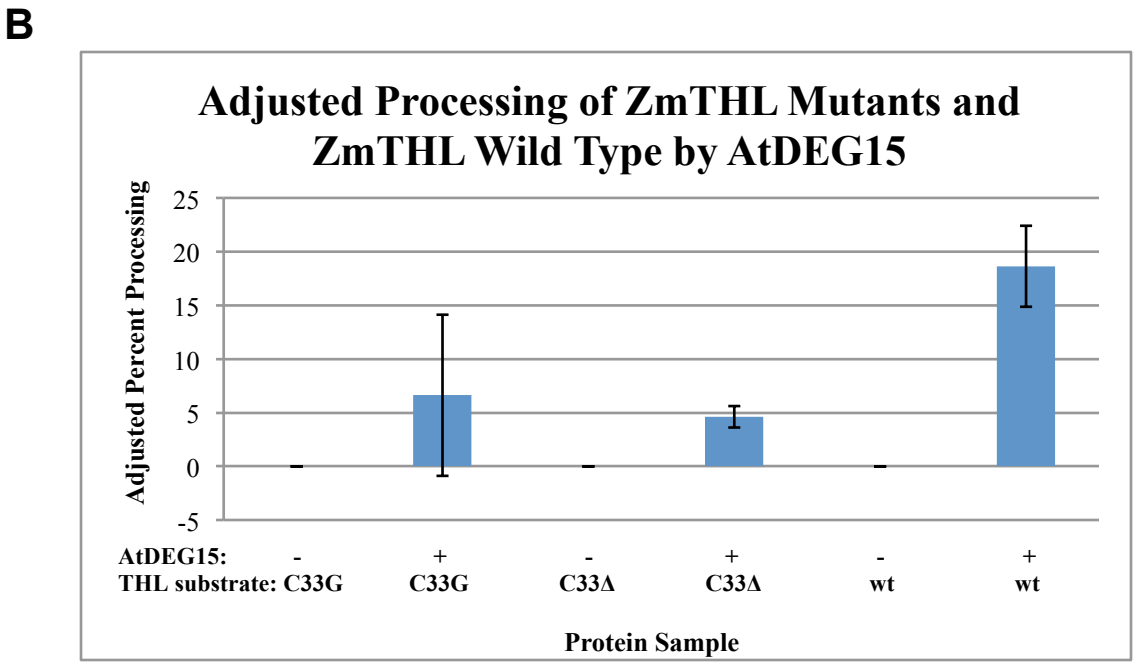

Figure 7: (A) One of three protease assays with ZmTHL C33G, ZmTHL C33Δ, and ZmTHL wild type (wt) and (B) quantification of the results of the three protease assays. Protease assays were repeated three times with AtDEG15 under the same conditions: 10 µg DEG15 was incubated with 250,000 cpm radioactively labeled THL for 4 hours at 37°C; 50,000 cpm loaded per lane; 3-night exposure. (-) indicates samples incubated with glass-distilled water instead of AtDEG15. (+) indicates samples incubated with AtDEG15. Blue bars represent the averages of the three protease assays. Error bars represent the standard error from the three protease assays. Adjusted percent processing refers to the percent processing after subtracting the percent processing of the negative control.

MATERIALS AND METHODS

Insertion of ZmTHL into pCR®II-TOPO®

Full-length *ZmTHL* cDNA, inserted in the EcoRV site of pCMV.SPORT-6.1, was obtained from the Arizona Genomics Institute (AGI). The *ZmTHL* cDNA was amplified by PCR and subsequently cloned using the TOPO TA Cloning® kit (Invitrogen). Transformants positive for gene insertion, as determined by blue-white screening, were grown in 3 mL of Luria broth containing kanomycin (1 μg/mL final). The plasmid DNA was isolated by a standard small-scale alkaline lysis protocol (Molecular Cloning). Finally, the correct construct, as determined by restriction digest screening and DNA sequencing, was purified by precipitation with PEG.

Site-Directed Mutagenesis

ZmTHL mutant constructs were made using the QuikChange® Site-Directed Mutagenesis Kit 5 from Stratagene. This kit utilizes the high-fidelity *PfuTurbo* DNA polymerase. The primers are shown in the table below. *ZmTHL C33G* PCR amplification conditions were as follows: initial denaturation, 30 s, 95˚C; denaturation, 30 s, 95˚C; annealing, 1 min, primer T_m-7; extension, 6 min, 68˚C; final extension, 1 min, 68˚C. The PCR amplification conditions for *ZmTHL C33*Δ were consistent with those of *ZmTHL C33G*, however, the annealing temperatures for the deletion mutant ranged from primer T_m-5 to T_m-9. The denaturation, annealing, and extension steps were cycled 16 times. After amplification, the plasmids were digested with *Dpn1*, a methylation-specific restriction enzyme, at 37˚C for 1 hour to digest the template DNA.

Primer	5'-3' Sequence
ZmTHL C33G Forward	GCGTCGGCGGGCGCGGCCGGG
ZmTHL C33G Reverse	CCCGGCCGCGCCCGCCGACGC
*ZmTHL C33*Δ Forward	CGGCGTCGGCGGCGGCCGGGG
*ZmTHL C33*Δ Reverse	CCCCGGCCGCCGCCGACGCCG

Table 1: Primers used in site-directed mutagenesis of *ZmTHL* gene. Primer names are indicated in the left column, beside their corresponding 5' to 3' sequence in the right column.

In vitro Transcriptions

Prior to transcription of RNA, 10 µL of plasmid DNA, diluted to 1mg/ml, was incubated with 20 units *SpeI* for 2 hours at 37˚C and purified by extraction with phenol-chloroform. 10 µL of the resulting linear DNA product (20 µL) was then transcribed under RNase-free conditions using 1.2 µL (20 units/µL) of T7 RNA polymerase (Promega) in 10 µL Transcription Optimized Buffer (Promega), 2.5 µL 1 mg/mL BSA, 5 µL 100 mM DTT, 10 µL 2.5 mM rNTPs, 3 µL 2.5 mM GTP, 5 µL 5 mM GpppG analog, and 0.5 µL 5 mM RNasin in a final volume of 50 µL. Transcriptions were incubated at 37˚C for 90 minutes. The mRNA was purified by extraction with phenol-chloroform and chloroform:isoamyl alcohol (24:1), and resuspended in 50 µL 10 mM DTT + 0.1 U/µL RNasin.

In vitro Translations

RNA was translated into protein using a cell-free lysate system wheat germ (Promega) containing ^{35}S-methionine (specific activity 43.5 TBq mmol^{-1}, MP Biochemicals). This mixture was incubated at room temperature for 90 minutes, after which 2.5 µL of unlabeled methionine were added to stop additional labeling of protein. Labeled protein was quantified by precipitation with TCA (trichloroacetic acid) using glass microfiber filters. An LS 6500 multi-purpose scintillation counter (Beckman) was used to determine the counts per minute (cpm) per µL.

Purification of AtDEG15 and ZmDEG15

Ali Dorchak purified *Arabidopsis thaliana* and *Zea mays* DEG15 by affinity chromatography with amylose resin. Protein concentration was determined by BCA protein assay in accordance with standard Olsen lab protocol.

DEG15 protease assays

Radioactive ZmTHL and mutants were diluted to 25,000 cpm/µL and radioactive AtTHL was diluted to 5000 cpm/µL. AtTHL appeared to show a much stronger signal, and therefore needed to be diluted further in attempts to equalize their appearance on a gel. 10 µL of each substrate were incubated with or without 5 µL 2 µg/µL DEG15 (protease species varied between experiments) in TYSND1 buffer (50 mM Hepes, pH 8.0, 115 mM NaCl, 0.2 mM DTT; Olsen Lab protocol; Kurochkin et al., 2007). All protease assays were incubated for 4 hours at 37˚C. After the 4 hour incubation, 50 µL 2x SDS-PAGE sample buffer (20% glycerol, 10% β-mercapto-ethanol, 4% SDS) was added and the samples were boiled at 100˚C for 5 minutes. Proteins were resolved by 10% SDS-PAGE and detected by x-ray film autoradiography.

Protease Assay Quantification

A Personal Molecular Imager® FX with Quantity One Quantitation Software and a phospho-screen were used to quantify the radioactive proteins. The percent processing was determined by dividing the amount of protein processed by the total protein present. Adjusted percent processing was determined by subtracting the negative control's percent processing from the percent processing of the samples with protease.

DISCUSSION

This study demonstrated that there is cross species enzyme activity. Although prior research had shown DEG15 processing of THL in *Arabidopsis thaliana* (Olsen lab unpublished results), these results indicate that processing occurs in *Zea mays*, as well. In fact, processing was most efficient when AtDEG15 and ZmTHL were incubated *in vitro*. These results support the conclusion that between these two species, ZmTHL is most efficiently processed and AtDEG15 is a more efficient protease. From these results, it can be gathered that homologous enzyme/substrate pairs are not necessary for efficient processing. On the contrary, this study showed that an *Arabidopsis thaliana* enzyme and a *Zea mays* substrate together had the highest levels of processing among the assay combinations. Therefore, DEG15 processing occurs across at least these two eukaryotic species.

According to the alignments of multiple PTS2-containing proteins, there is a conserved cysteine that could play a role in DEG15 recognition and PTS2 processing. *In vitro* protease assays that compared AtDEG15 processing of ZmTHL C33G and ZmTHL C33Δ revealed very little processing, if any. When the cysteine was mutated to a glycine, or deleted altogether, processing levels decreased significantly, indicating the PTS2 was not being cleaved. The results from this study support the hypothesis that the cysteine is a critical amino acid for DEG15 recognition and processing.

The amino acid sequence of ZmTHL was entered into the Protein Homology/analogy Recognition Engine V 2.0 (PHYRE2) to predict the three-dimensional structure of the protein (Figure 8). The processing site and the PTS2 signal that DEG15 recognizes is in the red region. The termini most likely move freely away

from the central globular part of the protein, allowing DEG15 to interact with the substrate. Preliminary models of the ZmTHL mutants did not show clear differences when compared to the wild-type model. It should be noted that PHYRE2 prediction results are only estimates and should be interpreted with caution.

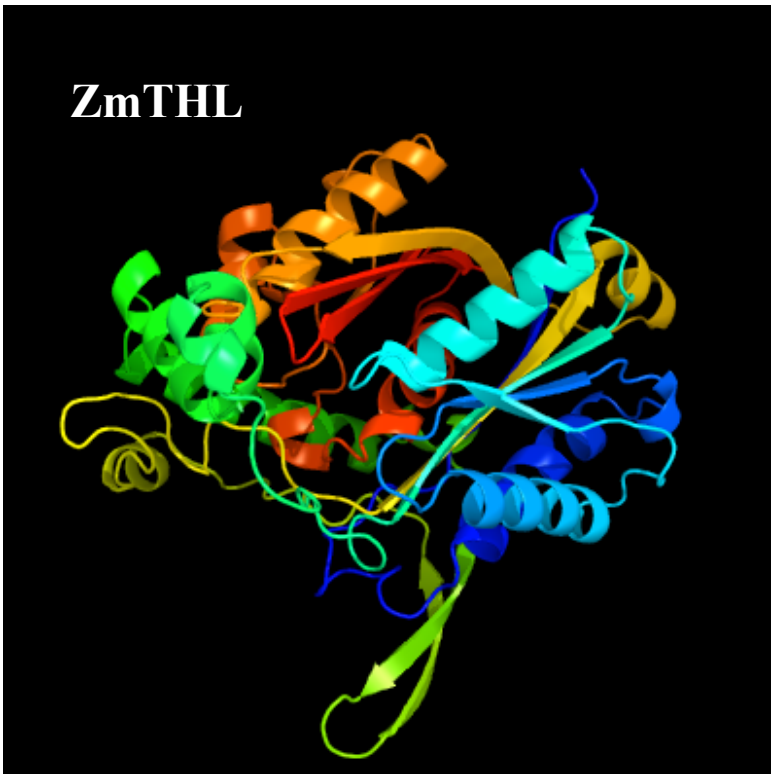

Figure 8: Three-dimensional structure of ZmTHL as predicted by PHYRE2 (intensive; Kelley and Sternberg, 2009). The protein is in rainbow order going from red (amino terminus) to blue (carboxyl terminus). The PTS2 and processing site are contained within the red regions of the protein.

With the conclusions from this study, it continues to be unclear whether DEG15 simply recognizes the conserved cysteine, or whether it recognizes a structural conformation of the protein that takes place around where the cysteine lies. This could explain why when the cysteine was mutated to a glycine, processing decreased, but was still not obliterated. However, when the cysteine was deleted, probably causing a greater

conformational change in the protein, processing levels decreased more noticeably. Conformational changes could affect the binding of the substrate to the enzyme, thereby decreasing processing by the protease. It would be interesting to alter the conformation of the substrate without mutating the cysteine to determine whether DEG15 recognizes conformational changes or the cysteine itself. If protease assays with a structurally modified ZmTHL wild type revealed decreased processing, it would appear that conformation plays a greater role in enzyme recognition than previously considered. By comparing processing levels of ZmTHL wild type and a ZmTHL wild-type sample that had a partially denatured conformation, this question could be addressed.

This study found that *Zea mays* thiolase, like *Arabidopsis thaliana* thiolase, is processed by DEG15. In future research, it would be interesting to see if PTS2 processing of thiolase is consistent across all higher eukaryotic species. Thiolase in *Triticum aestivum, Brachypodium distachyon,* or *Setaria italica* might be of interest in future research due to its sequence similarity to ZmTHL. If processing is indeed seen, it would be important to run a similar site-directed mutagenesis, as seen in this study, to determine whether the cysteine is consistently the site of DEG15 recognition. It would also be interesting to note whether AtDEG15 is more efficient than DEG15s of other species through various *in vitro* protease assays.

This project could be taken in another direction by examining the processing effects of DEG15 *in vivo*. Through confocal fluorescence microscopy in live plants, the process of protein localization into the peroxisome can be visualized. Furthermore, by fluorescently labeling the amino terminus without interfering with the PTS2 of thiolase, and also fluorescently labeling the carboxyl terminus of the protein, it can hopefully be

determined whether or not the PTS2 has been cleaved by DEG15 within the plant cell. With advanced technology, it could perhaps be noted that the two fluorescent labels on the protein separate upon entry into the peroxisome. Under this hypothesis, the fluorescent label on the carboxyl terminus would indicate the location of the mature protein, whereas the amino-terminal fluorescent label would portray the portion of the protein that has been proteolytically removed. This process would allow for comparison between the *in vivo* and *in vitro* techniques utilized. Using an *in vivo* approach would confirm DEG15 processing of thiolase actually occurs within various species and that *in vitro* protease assays reflect what happens physiologically within the plant.

The purpose of this study was to learn more about the peroxisome and add to the growing set of knowledge recently discovered about its functions. A better understanding of DEG15 recognition patterns in PTS2-containing proteins can help to further elucidate the biological role of processing of PTS2 proteins. The information gained from this study can hopefully serve as a stepping-stone for how to overcome peroxisomal disorders, especially those involving PTS2 proteins, in the future.

SUPPLEMENTARY INFORMATION

```
ZmTHL       MEKAIDRQRVLLAHLLPSPSAAS-SQPQLAASACAAGDSAAYQRSSSFGDDVVVVAAYRT 59
AtTHL       MEKAIERQRVLLEHLRPSSSSSHNYEASLSASACLAGDSAAYQRTSLYGDDVVIVAAHRT 60
            *****:****** ** **.*::   :..*:**** *********:* :*****:***:**

ZmTHL       PICKAKRGGFKDTYPEDLLTVVLKAVLDNTRINPADIGDIVVGTVLGPGSQRANECRMAA 119
AtTHL       PLCKSKRGNFKDTYPDDLLAPVLRALIEKTNLNPSEVGDIVVGTVLAPGSQRASECRMAA 120
            *:**:***.******:***: **:*::::*.:**:::**********.******.******

ZmTHL       LFAGFPETVPVRTVNRQCSSGLQAVADVAAAIKAGYYDIGIGAGLESMSINSIAWEGQVN 179
AtTHL       FYAGFPETVAVRTVNRQCSSGLQAVADVAAAIKAGFYDIGIGAGLESMTTNPMAWEGSVN 180
            ::*******.************************:***********: *.:****.**

ZmTHL       PKISAFQKAQDCLLPMGITSENVAHRYGVTRQEQDQAAAESHRRAAAATASGKFKDEIVP 239
AtTHL       PAVKKFAQAQNCLLPMGVTSENVAQRFGVSRQEQDQAAVDSHRKAAAATAAGKFKDEIIP 240
            * :. * :**:******:******:*:**:********.:***:******:*******:*

ZmTHL       VPTKIVDPKTGEEKEVVISVDDGIRPGTTASGLAKLKPVFKKDGTTTAGNSSQVSDGAGA 299
AtTHL       VKTKLVDPKTGDEKPITVSVDDGIRPTTTLASLGKLKPVFKKDGTTTAGNSSQVSDGAGA 300
            * **:******:** :.:******** ** :.*.**************************

ZmTHL       VLLMKRSVALKKGLPILGVFRSFAAVGVDPAVMGVGPAVAIPAAVKSAGLEIGDIDLFEL 359
AtTHL       VLLMKRSVAMQKGLPVLGVFRTFAAVGVDPAIMGIGPAVAIPAAVKAAGLELDDIDLFEI 360
            *********::****:*****:*********:**:**********:****:.******:

ZmTHL       NEAFASQFVYCCNKLGLDRSKVNVNGGAIALGHPLGATGARCVATLLNEMKRRGRDCRFG 419
AtTHL       NEAFASQFVYCRNKLGLDPEKINVNGGAMAIGHPLGATGARCVATLLHEMKRRGKDCRFG 420
            *********** ****** .*:******:*:****************:******:*****

ZmTHL       VVTMCIGSGMGAAAVFERGDAVDGLSNVRDIQAHNFLSKDAK- 461
AtTHL       VVSMCIGTGMGAAAVFERGDGVDELRNARKVEAQGLLSKDAR- 462
            **:****:************.** * *.*.::*:.:*****:

                        ZmTHL-AtTHL % IDENTITY: 77.44
```

Figure S1: ClustalW alignment of full length ZmTHL and AtTHL. PTS2 is highlighted in green. Conserved cysteine is highlighted in red. Percent identity comparison is shown at bottom.

ACKNOWLEDGEMENTS

First and foremost, I would like to thank Dr. Laura Olsen for giving me the opportunity to work in her lab and being a constant source of support, encouragement, and guidance throughout my undergraduate education. I would also like to thank my readers, Dr. Anuj Kumar and Dr. Amy Chang, for taking the time out of their busy schedules to read my thesis. I would like to thank Ali Dorchak and Kyle Helzer, for teaching and helping me along the entire journey—I could rely on your patience and sense of humor since my first day of training in the lab. I would also like to thank the other past and current members of the Olsen Lab that made each day in the lab a great experience, through their positive attitudes and constant support. I would especially like to thank Amish Desai, whose love and support everyday has helped me stay positive and smiling on even the most stressful days. Finally, I would like to thank my family, without whom none of this could have been possible. Thank you for always wanting the best for me and pushing me to achieve my goals.

REFERENCES

Cooper, G. M. (2000). Peroxisomes. Sinauer Associates. Retrieved from http://www.ncbi.nlm.nih.gov/books/NBK9930/

Crane, D. I., Maxwell, M. A., & Paton, B. C. (2005). PEX1 mutations in the Zellweger spectrum of the peroxisome biogenesis disorders. *Human Mutation*, *26*(3), 167–175. http://doi.org/10.1002/humu.20211

Dammai, V., & Subramani, S. (2001). The human peroxisomal targeting signal receptor, Pex5p, is translocated into the peroxisomal matrix and recycled to the cytosol. *Cell*, *105*(2), 187–96. Retrieved from http://www.ncbi.nlm.nih.gov/pubmed/11336669

Donaldson, R. P., Assadi, M., Karyotou, K., Olcum, T., & Qiu, T. (2001, May 30). Plant Cells: Peroxisomes and Glyoxysomes. In *Encyclopedia of Life Sciences*. Chichester, UK: John Wiley & Sons, Ltd.

Footitt, S., Cornah, J. E., Pracharoenwattana, I., Bryce, J. H., & Smith, S. M. (2007). The Arabidopsis 3-ketoacyl-CoA thiolase-2 (kat2-1) mutant exhibits increased flowering but reduced reproductive success. *Journal of Experimental Botany*, *58*(11), 2959–68. http://doi.org/10.1093/jxb/erm146

Gatto, G. J., Geisbrecht, B. V, Gould, S. J., & Berg, J. M. (2000). Peroxisomal targeting signal-1 recognition by the TPR domains of human PEX5. *Nature Structural Biology*, *7*(12), 1091–5. http://doi.org/10.1038/81930

Hayashi, Y., Sato, N., Shinozaki, A., & Watanabe, M. (2014). Increase in peroxisome number and the gene expression of putative glyoxysomal enzymes in Chlamydomonas cells supplemented with acetate. *Journal of Plant Research*, *128*(1), 177–185. http://doi.org/10.1007/s10265-014-0681-8

Helm, M., Lück, C., Prestele, J., Hierl, G., Huesgen, P. F., Fröhlich, T., … Gietl, C. (2007). Dual specificities of the glyoxysomal/peroxisomal processing protease Deg15 in higher plants. *Proceedings of the National Academy of Sciences of the United States of America*, *104*(27), 11501–6. http://doi.org/10.1073/pnas.0704733104

Hu, J., Baker, A., Bartel, B., Linka, N., Mullen, R. T., Reumann, S., & Zolman, B. K. (2012). Plant peroxisomes: biogenesis and function. *The Plant Cell*, *24*(6), 2279–303. http://doi.org/10.1105/tpc.112.096586

Johnson, T. L., & Olsen, L. J. (2001). Building New Models for Peroxisome Biogenesis. *PLANT PHYSIOLOGY*, *127*(3), 731–739. http://doi.org/10.1104/pp.010262

Kelley, L.A. and Sternberg, M.J.E. (2009) Protein structure prediction on the web: a case study using the Phyre server. *Nature Protocols* 4, 363 – 371.

Kurochkin, I. V, Mizuno, Y., Konagaya, A., Sakaki, Y., Schönbach, C., & Okazaki, Y. (2007). Novel peroxisomal protease Tysnd1 processes PTS1- and PTS2-containing enzymes involved in beta-oxidation of fatty acids. *The EMBO Journal*, *26*(3), 835–45. http://doi.org/10.1038/sj.emboj.7601525

Lodish, H., Berk, A., Zipursky, S. L., Matsudaira, P., Baltimore, D., & Darnell, J. (2000). Synthesis and Targeting of Peroxisomal Proteins. W. H. Freeman. Retrieved from http://www.ncbi.nlm.nih.gov/books/NBK21520/

Ma, C., Agrawal, G., & Subramani, S. (2011). Peroxisome assembly: matrix and membrane protein biogenesis. *The Journal of Cell Biology*, *193*(1), 7–16. http://doi.org/10.1083/jcb.201010022

Nelson, D. L., Lehninger, A. L., & Cox, M. M. (2008). *Lehninger Principles of Biochemistry*. W. H. Freeman. Retrieved from https://books.google.com/books?hl=en&lr=&id=5Ek9J4p3NfkC&pgis=1

Schuhmann, H., Huesgen, P. F., Gietl, C., & Adamska, I. (2008). The DEG15 serine protease cleaves peroxisomal targeting signal 2-containing proteins in Arabidopsis. *Plant Physiology*, *148*(4), 1847–56. http://doi.org/10.1104/pp.108.125377

Waterham, H. R., & Ebberink, M. S. (2012). Genetics and molecular basis of human peroxisome biogenesis disorders. *Biochimica et Biophysica Acta (BBA) - Molecular Basis of Disease*, *1822*(9), 1430–1441. http://doi.org/10.1016/j.bbadis.2012.04.006